



Mechanical strain and damage in Si implanted with O and N ions at elevated temperatures: Evidence of ion beam induced annealing

J. P. de Souza, Yu. Suprun-Belevich, H. Boudinov, and C. A. Cima

Citation: [Journal of Applied Physics](#) **89**, 42 (2001); doi: 10.1063/1.1330254

View online: <http://dx.doi.org/10.1063/1.1330254>

View Table of Contents: <http://scitation.aip.org/content/aip/journal/jap/89/1?ver=pdfcov>

Published by the [AIP Publishing](#)



Re-register for Table of Content Alerts

Create a profile.



Sign up today!



Mechanical strain and damage in Si implanted with O and N ions at elevated temperatures: Evidence of ion beam induced annealing

J. P. de Souza, Yu. Suprun-Belovich, and H. Boudinov

Instituto de Física, Universidade Federal do Rio Grande do Sul, 91501-970, Porto Alegre, R.S., Brazil

C. A. Cima^{a)}

PGCIMAT, Universidade Federal do Rio Grande do Sul, 91501-970, Porto Alegre, R.S., Brazil

(Received 6 July 2000; accepted for publication 6 October 2000)

The accumulation of damage and the development of mechanical strain in crystalline Si (*c*-Si) by O and N ion implantation to doses up to $4 \times 10^{17} \text{ cm}^{-2}$ at elevated temperatures have been studied using Rutherford backscattering spectrometry and high resolution x-ray diffraction. The implantation of O or N ions at high temperatures produces two distinct layers in the implanted *c*-Si: (i) a practically damage-free layer extending from the surface up to \approx half of the depth of the mean projected range (R_p) and presenting negative strain (of contraction); and (ii) a heavily damaged layer located around and ahead of the R_p with no significant strain. Both the damage distribution and the magnitude of the strain were found to be dependent on the ion species implanted. We proposed that besides the spatial separation of Frenkel pair defects due to the mechanics of the collision processes and the intensive dynamic annealing, an ion beam induced annealing process also participate in the formation of the near-surface damage-free layer during high temperature implantation of *c*-Si. © 2001 American Institute of Physics. [DOI: 10.1063/1.1330254]

I. INTRODUCTION

It is generally accepted that residual implantation damage in crystalline Si (*c*-Si) decreases with increasing temperature of the implantation. Below $\sim 200^\circ\text{C}$, the damage accumulation from light or medium mass ions results in the formation of an amorphous layer at sufficiently high doses, while above this temperature, the crystalline-to-amorphous transformation does not take place up to arbitrarily high doses.¹ High dose implantation has been used to synthesize a variety of compounds in silicon including a buried oxide layer and a buried nitride layer for silicon-on-insulator (SOI) device applications. Ion implantation at elevated temperatures provides a possibility for exploring damage-related phenomena at very high doses.²⁻⁵ Understanding of the mechanisms of the growth of damage ion implantation at high dose and elevated temperatures is of great importance for the synthesis of SOI materials.

It was previously found that the implantation of *c*-Si at elevated temperatures with O ions leads to a damage accumulation which was shown to bifurcate into two distinctly different layers: a heavily dislocated region around and ahead of the mean projected range (R_p), and a shallower layer which is dislocation free but shows mechanical strain of contraction in the planes parallel to the surface.^{2,3,6,7} The role of the impurity atoms in the growth of the damage is not clear at present and detailed information on the damage growth during implantation of Si with ions other than those of O and Si at elevated temperatures is scarcely discussed in the literature.

In this paper, we present the results of systematic investigations of damage accumulation and evolution of internal

mechanical strain at high temperature and high dose implantation of *c*-Si with O or N ions. The influence of the implanted species on the process of the formation of the layer with a negative strain and on the damage accumulation has been investigated.

II. EXPERIMENTAL DETAIL

Czochralski-grown silicon wafers of *n*-type conductivity, with resistivity of 1–2 $\Omega \text{ cm}$ and (100) orientation were implanted at temperatures from 150 to 600 $^\circ\text{C}$ with molecular ions (N_2^+ or O_2^+) of 240 keV, which corresponds to the energy of 120 keV/atom. At the higher energy of 185 keV the implantation was performed using $^{16}\text{O}^+$ ions. The beam current density was maintained in the range of 3–6 $\mu\text{A cm}^{-2}$. The implanted doses (atom/cm^2) were chosen in the range of $0.5\text{--}4.0 \times 10^{17} \text{ cm}^{-2}$. The estimated R_p values from TRIM⁸ code simulation are 0.26 and 0.27 μm , respectively, for 120 keV O and N ions, and 0.37 μm for the 185 keV O ions. In order to reduce channeling effects, the normal of the samples was tilted by 7° with respect to the beam direction and the surface was rotated by 25° with respect to the $\langle 110 \rangle$ direction.

The implanted samples were analyzed by Rutherford backscattering spectrometry (RBS) using a 900 keV $^4\text{He}^+$ beam aligned with $\langle 100 \rangle$ crystal direction or in random direction. The depth profiles of the damage were obtained from the RBS spectra using an iterative calculation procedure with the two dechanneled beams' approximation.⁹

Internal mechanical strain in the samples was investigated by high-resolution x-ray diffraction measurements in double-axis and triple-axis configurations using a $\text{Cu K}\alpha_1$ beam. By measuring the angular distance between the diffraction peaks from the Si substrate and the implanted layer

^{a)}Electronic mail: alcima@if.ufrgs.br

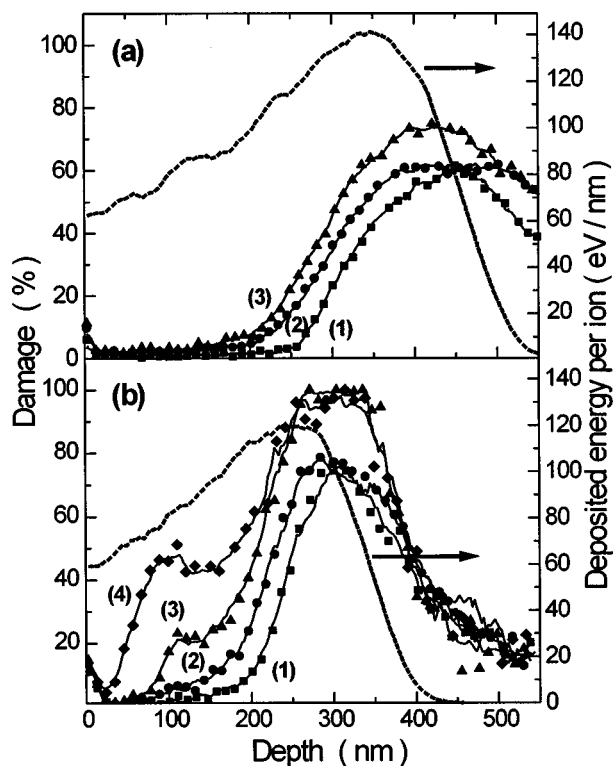


FIG. 1. Damage profiles extracted from the RBS spectra from Si implanted at 600 °C. (a) 185 keV O ions, doses: (1) $5 \times 10^{16} \text{ cm}^{-2}$; (2) $2 \times 10^{17} \text{ cm}^{-2}$; (3) $4 \times 10^{17} \text{ cm}^{-2}$. (b) 120 keV N ions, doses: (1) $1 \times 10^{17} \text{ cm}^{-2}$; (2) $2 \times 10^{17} \text{ cm}^{-2}$; (3) $3 \times 10^{17} \text{ cm}^{-2}$; (4) $4 \times 10^{17} \text{ cm}^{-2}$. The corresponding energy deposited in nuclear collisions calculated by TRIM is shown by the dashed curves.

in the (004) orientation in the rocking curves, the relative perpendicular mismatch $(\Delta d/d)_{\perp}$ was obtained. The in-plane component of the strain was found to be negligible in all the cases by examination of the reflections from the inclined lattice planes. To obtain the information about the depth distribution of the damage the measurements were repeated after the surface of the samples had been etched to a certain depth.

III. EXPERIMENTAL RESULTS

The depth distributions of the damage obtained from the RBS spectra of the samples implanted with O (of 185 keV) and N ions (of 120 keV/atom) at 600 °C to various doses are presented in Figs. 1(a) and 1(b), respectively. 100% of the damage indicated in the figures corresponds to the “random level” or 100% of dechanneling. The corresponding depth profiles of the energy deposited by the projectile ions, calculated using the TRIM code simulation,⁸ are included in Figs. 1(a) and 1(b) for comparison. It was verified by RBS analysis (data not shown) that the damage profile after room temperature (RT) implantation with either O or N ions to doses below the threshold dose for amorphization has its maximum at a depth which closely coincides with that of the deposited energy distribution. It is clearly apparent in Figs. 1(a) and 1(b) that the damage profiles produced by implantation at elevated temperatures are shifted to deeper depths with re-

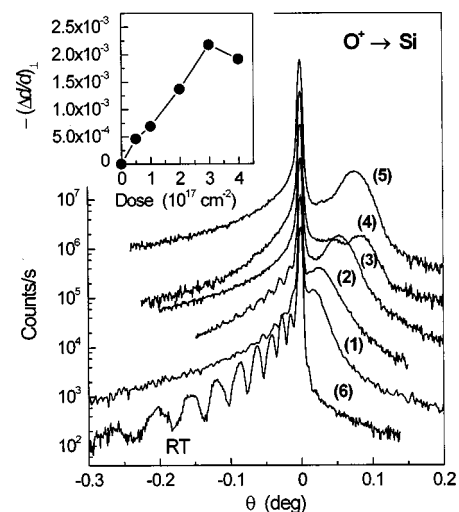


FIG. 2. X-ray rocking curves from Si implanted at 600 °C with 185 keV O ions. Doses: (1) $5 \times 10^{16} \text{ cm}^{-2}$; (2) $1 \times 10^{17} \text{ cm}^{-2}$; (3) $2 \times 10^{17} \text{ cm}^{-2}$; (4) $3 \times 10^{17} \text{ cm}^{-2}$; (5) $4 \times 10^{17} \text{ cm}^{-2}$. (6) RT implantation, dose $2 \times 10^{15} \text{ cm}^{-2}$. The obtained negative strain vs the dose is shown in the inset.

spect to the deposited energy distribution, meaning that the damage is accumulated at depths deeper than at RT implantation

According to the RBS studies there is a near-surface layer practically free of damage in the samples implanted with O ions at elevated temperatures. No amorphous layer is observed in samples implanted with O ions and the damage profile practically does not alter with the dose. The data in Fig. 1(b) show that in the samples implanted with N ions with dose $\geq 3 \times 10^{17} \text{ cm}^{-2}$ a thin buried amorphous like layer is formed, which becomes thicker with the dose. Additionally, the near-surface damage-free layer in the samples is narrower than those implanted with O ions. For the highest N dose ($4 \times 10^{17} \text{ cm}^{-2}$) the near-surface damage-free layer is practically missing. On the damage profiles in the samples implanted with N ions to doses of $2 \times 10^{17} \text{ cm}^{-2}$ and above there is an additional maximum or shoulder starting at the depth of 100–120 nm.

Figure 2 shows the rocking curves [curves (1)–(5)] from the samples implanted at 600 °C with 185 keV O ions to various doses. A rocking curve from a sample implanted at RT with O ions to a dose of $2 \times 10^{15} \text{ cm}^{-2}$ (below the onset for amorphization) is included for comparison [curve (6)]. In curve (6) the fringes to the left of the main peak indicate the presence of a positive strain (of expansion), which is normally observed in *c*-Si after RT implantation. The rocking curves from the samples implanted at 600 °C show a large substrate reflection peak and a secondary peak to the right of the main peak [see curves (1)–(5) in Fig. 2]. This secondary peak indicates that there is a crystal layer in the samples with negative lattice strain (of contraction). The strain perpendicular to the surface $(\Delta d/d)_{\perp}$ obtained from the x-ray measurements versus the O ion dose is shown in the inset in Fig. 2. There is a maximum of the negative strain at the dose of $3 \times 10^{17} \text{ cm}^{-2}$.

The rocking curves obtained from the samples implanted at 600 °C with N ions (at 120 keV/atom) to various doses are

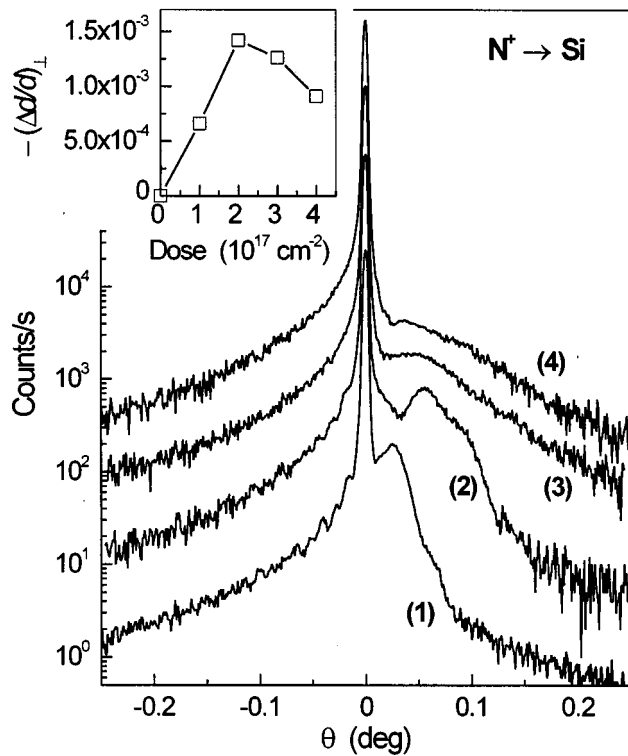


FIG. 3. X-ray rocking curves from Si implanted at 600 °C with 120 keV N ions. Doses: (1) $1 \times 10^{17} \text{ cm}^{-2}$; (2) $2 \times 10^{17} \text{ cm}^{-2}$; (3) $3 \times 10^{17} \text{ cm}^{-2}$; (4) $4 \times 10^{17} \text{ cm}^{-2}$. The obtained negative strain vs the dose is shown in the inset.

shown in Fig. 3. The strain $(\Delta d/d)_{\perp}$ calculated from the x-ray measurements versus the N dose is shown in the inset in Fig. 3. There is an increase of the strain with the increase of the dose up to $2 \times 10^{17} \text{ cm}^{-2}$. With the further increase of the dose the strain significantly decreases.

Controlled etching of the surface of the samples with subsequent recurring x-ray measurements demonstrated that the negatively strained region extends from the surface up to the depth of $\approx R_p/2$. The crystal layer around and ahead of R_p does not show any noticeable strain.

Figure 4 shows the damage profiles after implantation of O ions (at 120 keV/atom) with a fixed dose of $1 \times 10^{17} \text{ cm}^{-2}$, at various temperatures. At the lowest temperature (150 °C) a 230-nm-thick buried amorphous layer centered at the depth corresponding to that of the maximum energy deposition is formed [curve (1) in Fig. 4]. However, even at this temperature a thin layer with a very low damage concentration is observed near the surface. With the increase of the implantation temperature the amorphous layer becomes thinner, however, it is still centered at the same depth (curve 2 in Fig. 4). No amorphous layer is observed after implantation at higher temperatures, and the damage profile is shifted to deeper depths [curves (3) and (4) in Fig. 4].

The strain calculated from the x-ray curves versus the temperature of the implantation in samples which received an O ion dose of $1 \times 10^{17} \text{ cm}^{-2}$ at the energy of 120 keV/atom is displayed in Fig. 5. One can notice that the negative strain decreases with increasing implantation temperature from 150 °C.

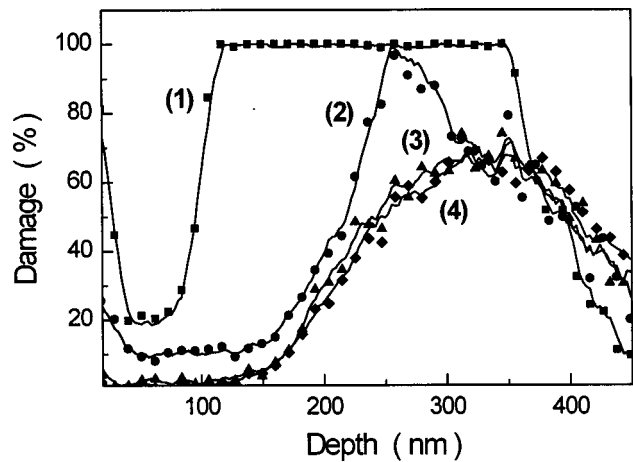


FIG. 4. Damage profiles extracted from the RBS spectra from Si implanted with 120 keV O ions, dose $1 \times 10^{17} \text{ cm}^{-2}$. Implantation temperatures: (1) 150; (2) 200; (3) 400; (4) 600 °C.

IV. DISCUSSION

The damage accumulation and distribution along the depth observed for high temperature implantation of O ions is in accordance with the results reported in the literature.^{2,6} There are two distinct damage layers in the implanted material. The near-surface layer has a very low damage concentration, since the backscattering yield in the aligned RBS spectra from this layer closely coincides with that in a virgin sample. In addition, this layer presents unidirectional strain of lattice contraction (Fig. 2). However, the buried damaged layer located around and ahead of the R_p of the ions (Fig. 1) presents no significant induced strain as verified via rocking curve measurements performed after removal of the near-surface layer by controlled chemical etch. Similar results were also observed in Si implanted with Si ions.^{2,4} A model was previously proposed to explain the formation of these two layers based on a spatial separation of Frenkel interstitial-vacancy pairs created during irradiation.^{2,4} The momentum transferred to the recoiled Si interstitial atoms should have a nonzero component along the direction of the incident ion beam. Consequently, a spatial separation between the interstitial and vacancy defects, with the interstitial

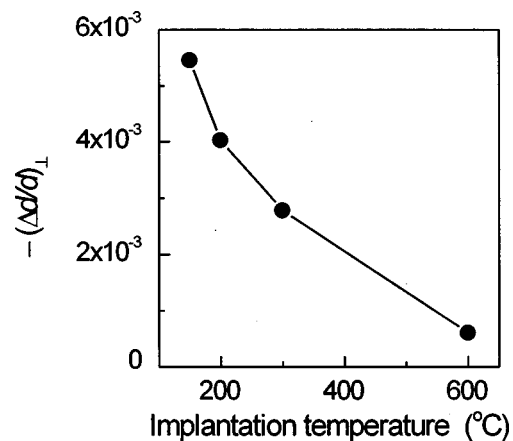


FIG. 5. Strain vs the implantation temperature for Si implanted with 120 keV O ions, dose $1 \times 10^{17} \text{ cm}^{-2}$.

Si atoms distributed to greater depth on average, is produced. Thus, the excess concentration of vacancies, mainly located near the surface, forms vacancy-type defect clusters which induce the observed negative strain. On the other side, the excess concentration of interstitial Si atoms located around and ahead of the R_p of the ions promotes the formation of extended defects. The suggested model² was supported by the results of calculations of vacancy and interstitial Si atom distributions using a special modified version of TRIM.

In the present research, generally similar results were obtained in samples implanted with O and N ions. However, compared to O ions, N ions produce a higher level of damage around R_p causing the higher backscattering yield observed over this region. In addition, at doses of $3 \times 10^{17} \text{ cm}^{-2}$ and higher a buried amorphous like layer is formed [see curves (3) and (4) in Fig. 1(b)]. Besides that, there is an additional maximum or a shoulder on the damage profile between the two layers at doses $\geq 2 \times 10^{17} \text{ cm}^{-2}$, indicating that some specific mechanism of defect-impurity interaction is taking place. A similar disordered layer on the interface between the Si crystal layer and buried Si_3N_4 layer was observed in previous works.¹⁰ The negative strain generated by N ion implantation to doses up to $2 \times 10^{17} \text{ cm}^{-2}$ is higher than that produced by O ions for the same implantation parameters, in spite of the fact that the mass of N ions is lighter than that of O ions. Our earlier experiments employing other light mass ions implanted at high temperatures showed that the formation of the near-surface layer of negative strain cannot be explained solely by the collision mechanics and it was suggested that chemical properties of the implanted species should play a role in the damage accumulation process at elevated temperatures.¹¹

It is seen from Fig. 4 that at relatively low temperature (150 °C) there is a buried amorphous layer formed by the O ion implantation, and the near-surface layer with the negative strain is rather thin ($\sim 100 \text{ nm}$). However, in this case the magnitude of the negative strain is the highest (Fig. 5). With the increase of the temperature the thickness of the near-surface layer increases and the strain decreases. This effect is difficult to explain using the model suggested in Refs. 2 and 4, which consider only the spatial separation of the Frenkel pair defects. Some additional mechanisms may be involved to assist the formation of the above-mentioned double-layer structure.

We propose that during high temperature implantation intense annealing of defects takes place in the near-surface region. In addition to the dynamic annealing of point defects, energy of the incoming ions are transferred to Si atoms pertaining to previously created defect structures. Eventually, Si atoms displaced from the defect structures occupy regular lattice positions after filling vacancy sites. The beam assisted transfer of Si atoms from defect structures to regular lattice sites is referred to hereafter as ion beam induced annealing (IBIA). As a consequence of the IBIA, the formation of extended defect structures from the accumulation of interstitial Si atoms is prevented in the near-surface region, giving origin to the damage-free near-surface layer. Beyond the near-surface layer the IBIA is expected to be attenuated because the energy depositing in those regions is not sufficient to

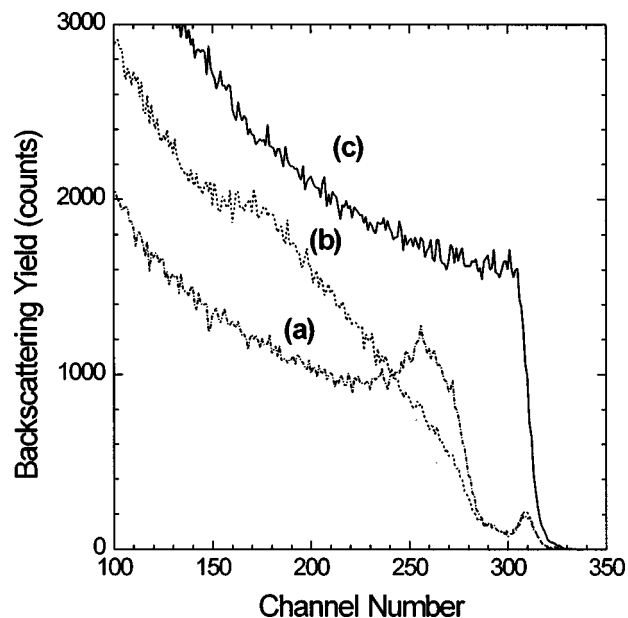


FIG. 6. (a) (100) aligned spectrum of a sample implanted at 500 °C with O ions to the dose of $2 \times 10^{16} \text{ cm}^{-2}$ and energy of 50 keV; (b) (100) aligned spectrum of the same sample after a second implantation at the same temperature, with O ions at 185 keV and dose of $1 \times 10^{17} \text{ cm}^{-2}$; and (c) random RBS spectrum of the same sample after the dual O ion implantation.

avoid the buildup of stable defect structures. In addition, the presence of a high concentration of O or N atoms around the R_p region markedly reduces the dynamic annealing.^{12,13} There are also additional interstitial Si atoms created in this region to accommodate the volume expansion due to formation of impurity precipitates. Consequently, during high temperature implantation the damage is accumulated mainly beyond the depth where the maximum energy deposition occurs ($\cong 0.8R_p$). The damage in those regions is composed mainly of extended defect structures and silicon oxide or silicon nitride precipitates, which are stable up to extremely high temperatures ($> 1200 \text{ °C}$). In the case of N ion implantation, the crystal at the end of range region is heavily disordered or amorphous like. For high N ion doses, like $4 \times 10^{17} \text{ cm}^{-2}$, the N concentration may initiate a Si_3N_4 phase formation. The lower fraction of N necessary for the formation of Si_3N_4 , than of O for the formation of SiO_2 , may explain the difference in the behavior of the observed damage accumulation over the R_p region with an increasing N ion dose [see Fig. 1(b)].

In order to demonstrate the IBIA phenomenon, a separate experiment was conducted employing dual O ion implantation at a temperature of 500 °C. The first implantation was performed with a dose of $2 \times 10^{16} \text{ cm}^{-2}$ and energy of 50 keV/atom to create a buried defect structure centered at the depth of $\cong 0.15 \text{ }\mu\text{m}$. Subsequently, half of the sample surface was protected with a mechanical mask and a second O implantation was performed at a higher energy of 120 keV/atom with a dose of $1 \times 10^{17} \text{ cm}^{-2}$.

Curves (a) and (b) in Fig. 6 are, respectively, the aligned RBS spectra taken from the single and dually O ion implanted halves of the sample. For comparison, the random RBS spectrum is included in Fig. 6 [curve (c)]. The regions

comprising channels 245–280 in curves (a) and (b) correspond to the backscattering from the damage introduced by the first O ion implantation. Since over this region the backscattering yields in curve (b) are lower than those in curve (a) it is reasonable to conclude that the higher energy implantation annealed part of the original damage. Considering that the end of range defects created by elevated temperature implantation are stable up to very high temperature treatments (>1000 °C), the hypothesis of defect annealing due to the temperature of the wafer has been excluded. Further investigation demonstrated that the damage distributions produced by the lower energy O ion implantation in a virgin *c*-Si and in a *c*-Si previously implanted with the higher energy O are identical. Quite similar results were obtained by replacing the O for N in the higher energy ion implantation (data not shown). The obtained results constitute clear evidence of the IBIA phenomenon.

As the negative strain in the near-surface layer does not develop after RT implantation or even after a relatively low dose implantation at elevated temperatures,⁶ we can assume that the formation of the vacancy clusters is the peculiar result of the defect annealing during the high temperature and high dose implantation. It is expected that the increase of the implantation temperature enhances the dynamic annealing of the point defects, resulting in the formation of a lower number of vacancy clusters and therefore explaining the observed decrease of the negative strain (Fig. 5). The growth of the strain with the dose in the O ion implanted samples shows a saturation and a decay after the dose of $3 \times 10^{17} \text{ cm}^{-2}$ (Fig. 2, inset), indicating some limit of the crystal lattice to accommodate the growing number of vacancies. On the other hand, at very high doses ($4 \times 10^{17} \text{ cm}^{-2}$) mechanisms for strain relaxation become operative. One possible mechanism is strain relaxation by generation of a dislocation band imbedded in the near-surface region.³ In the case of implantation of N ions the drastic decay of the negative strain at doses $>2 \times 10^{17} \text{ cm}^{-2}$ (Fig. 3) occurs simultaneously with the formation of disturbances of the crystal lattice in the near surface layer [Fig. 1(b)]. At the dose of $4 \times 10^{17} \text{ cm}^{-2}$ the damage-free surface layer is almost completely eliminated, which is accompanied by a cutting drop of the negative strain (Fig. 3, inset).

V. CONCLUSIONS

The results obtained in the present investigation suggest that the model of spatial separation of interstitial Si atoms and vacancies^{2,5} does not completely explain the damage and strain buildup in *c*-Si by O or N ion implantation. It was

found that besides the lighter mass of N compared to O, the implantation of N ions produces higher mechanical strain and higher damage than O ions. This seems to indicate that the implanted species participate in the damage formation during the implantation at elevated temperatures.

We proposed that in addition to the spatial separation of the Frenkel pairs and intensive dynamic annealing occurring during implantation at elevated temperatures, the IBIA participates actively in the formation of the near-surface weakly damaged layer. In regions around R_p , where a high concentration of implanted O or N atoms is present, the dynamic annealing is significantly reduced. Considering the efficiency of the IBIA process proportional to the energy deposited by the beam one expects that it should decrease abruptly for depths beyond that of the maximum energy deposition ($\cong 0.8R_p$). Consequently, the damage builds up mainly at the end of range of the ions. The presented rationale explains the observed shift of the damage profile toward the depth in *c*-Si implanted with O or N ions at high temperatures.

ACKNOWLEDGMENTS

This research was partly supported by Fundação de Amparo à Pesquisa do Estado do Rio Grande do Sul (FAPERGS), Conselho Nacional de Desenvolvimento Científico e Tecnológico (CNPq), and Financiadora de Estudos e Projetos (Finep).

¹F. F. Morehead, B. L. Crowder, and R. S. Title, *J. Appl. Phys.* **43**, 1112 (1972).

²O. W. Holland, J. D. Budai, and B. Nielsen, *Mater. Sci. Eng., A* **253**, 240 (1998).

³O. W. Holland, D. S. Zhou, and D. K. Thomas, *Appl. Phys. Lett.* **63**, 896 (1993).

⁴O. W. Holland and C. W. White, *Nucl. Instrum. Methods Phys. Res. B* **59/60**, 353 (1991).

⁵D. Venables and K. S. Jones, *Nucl. Instrum. Methods Phys. Res. B* **74**, 65 (1993).

⁶D. Venables, K. S. Jones, F. Namavar, and J. M. Manke, *Mater. Res. Soc. Symp. Proc.* **235**, 103 (1992).

⁷S. L. Ellingboe and M. C. Ridgway, *Nucl. Instrum. Methods Phys. Res. B* **127/128**, 90 (1997).

⁸J. F. Ziegler, J. P. Biersack, and U. Littmark, *The Stopping and Ranges of Ions in Solids* (Pergamon, New York, 1985).

⁹F. Eisen, in *Channeling*, edited by D. V. Morgan (Wiley, New York, 1973), p. 417.

¹⁰C. D. Meekison, G. R. Booker, K. J. Reeson, P. L. F. Hemment, R. F. Peart, B. J. Chater, J. A. Kilner, and J. R. Davis, *J. Appl. Phys.* **69**, 3503 (1991).

¹¹J. P. de Souza, Yu. Suprun-Belovich, H. Boudinov, and C. A. Cima, *J. Appl. Phys.* **87**, 8385 (2000).

¹²E. F. Kennedy, L. Csepregi, J. W. Mayer, and T. W. Sigmon, *J. Appl. Phys.* **48**, 4241 (1977).

¹³H. Boudinov and J. P. de Souza, *Nucl. Instrum. Methods Phys. Res. B* **122**, 293 (1997).